Modeling the Behavior of Frost Growth on Finned Tube Heat Exchanger

Dr.Zainab Hasoun H.Naji
Machine and Equipment Engineering Department, University of Technology/Baghdad
Email: Dr-z-alnaji @yahoo.com

Received on: 23/9/2012 & Accepted on: 11/6/2013

ABSTRACT

A quasi-steady finite-volume model was developed for modeling a plain-fin-round-tube heat exchanger under frosted conditions. In this study, the heat and mass transfer characteristics of heat exchangers during frost formation process are analyzed numerically. Unsteady heat and mass transfer coefficients of the air side, heat transfer coefficient of the refrigerant side, frost layer thickness, the surface efficiency of the heat exchanger and the mass flow rate of the frost accumulated on the heat exchanger surface are calculated. The total conductivity (UA) and pressure drop of the heat exchanger are reported for different air inlet and refrigerant temperature. Results have shown that frost layer growth is faster with lower inlet air temperature. Using the developed mathematical model, the algorithm and the computer code, which have been experimentally validated, it is possible to predict a decrease of exchanged heat flux in the heat exchanger under frost growth conditions. The model could be further extended to simulate direct expansion evaporators with varying operating conditions and variable heat exchanger geometry.

Keywords: Finned Tube; Modeling; Frost Formation; Heat Transfer; Mass Transfer.

نمذجة تصرف نمو الصقيع على مبادل حراري ذو زعانف

الخلاصة

تم استخدام طريقة الحجوم الثابتة لنمذجة مبادل حراري ذو زعانف مستوية تحت ظروف نمو الصقيع عليه. في هذه الدراسة, تم تحليل خصائص انتقال الكتلة والحرارة للمبادل الحراري خلال عملية تكون الصقيع عليه كما تم حساب معاملات انتقال الحرارة والكتلة الغير مستقرة لجانب الهواء, ومعامل انتقال الحرارة لجانب مائع التبريد, وكفاءة سطح المبادل الحراري, ومعدل تدفق الكتلة للصقيع المتراكم على سطح المبادل الحراري. وكذلك المعامل الكلي للتوصيل(UA) وهبوط الضغط للمبادل الحراري تم حسابها عند درجات حرارة مختلفة للهواء الداخل وكذلك لمائع التبريد. وقد اظهرت النتائج ان طبقة الثلج تنمو اسرع عند زيادة درجة حرارة الهواء الداخل. تم بناء برنامج حاسوبي لتمثيل المسألة رياضيا والذي اثبت فعاليته عند مقارنته مع النتائج العملية, وقد وجد من خلاله انه من الممكن التنبؤ بالنقصان في معدل انتقال الحرارة للمبادل الحراري تحت ظروف نمو الصقيع. والنموذج الحالي يمكن ان يتسع ليشمل حساب مبخرات التمدد المباشرة مع تغير ظروف التشغيل وكذلك تغير الشكل الهندسي للمبادل الحراري.

https://doi.org/10.30684/etj.32.1A.16
2412-0758/University of Technology-Iraq, Baghdad, Iraq

NOMENCLATURE

A_f fin surface area [m^2]
A_i inner surface area of evaporator [m^2]
A_{min} minimum air flow area [m^2]
A_o total heat transfer area [m^2]
cp specific heat of air at constant pressure [$kJkg^{-1}K^{-1}$]
D diameter[m]
f friction factor [-]
G_{max} Maximum mass flux [kg m^{-2} s^{-1}]
ha Air side heat transfer coefficient [W m_2 K_1]
hr refrigerant heat transfer coefficient [W m^{-2} K^{-1}]
j Colburn's dimensionless heat transfer coefficient
k_{fr} thermal conductivity of frost [(kW m^{-1} K^{-1}]
k_a Thermal conductivity of air [W m^{-1} K^{-1}]
Le Lewis number[-]
m_{fr} frost deposition rate [kg s^{-1}]
m_{air} air mass flow rate [kg s^{-1}]
m_k fin parameter[-]
N_{fin} number of fins [-]
Pr Prandtl number [-]
Q load [kW]
Re Reynolds number [-]
S_L longitudinal tube spacing [m]
S_T transverse tube spacing [m]
t time [s]
T temperature [°C]
UA the overall heat transfer coefficient of heat exchanger [W m^{-2} K^{-1}]
w air absolute humidity [kg_{water}/kg_{air}]
W width of heat exchanger [m]

Greek symbols

δ_{fr} frost thickness [m]
ΔP Air side pressure drop [Pa]
Δh_{sg} enthalpy of formation of ice
ρ_i density of ice [kg m^{-3}]
ρ_{fr} density of frost [kg m^{-3}]
ρ_e density of air at air flow outlet [kgm^{-3}]
ρ_i density of air at air flow inlet [kg m^{-3}]
ρ_m density of air calculated at average
Temperature of air inlet and outlet [kg m^{-3}]
ρ_{ice} ice density [kg m^{-3}]
η_f fin efficiency
η_s surface efficiency
σ minimum flow area/face area

Subscripts

a, air
amb, evaluated at ambient air temperature

av, evaluated at average inlet and outlet conditions
average averaged over the entire heat exchanger
dry, corresponding to unfrosted conditions
fr , frost
in, inlet
max, maximum
o, overall (fin and tube)
out, outlet
r, refrigerant
sens, sensible
si , base of the fin (i.e. tube outer surface)
so , frost surface (fin or tube)
th ,thickness

INTRODUCTION

Moist air passes over a surface at temperatures below the dew temperature of the air, some of its vapor content will be condensed on the surface. If the surface temperature is below the 0°C, vapor will be deposited first as water droplets which subsequently freeze and, if the temperature is less than about -50C, a porous structure of ice crystals forms. This layer of ice crystals is known as frost.

Frost growth on heat exchanger surfaces reduces the airflow through the heat exchangers and increases the air pressure drop through heat exchangers. Eventually, after many hours of frost growth, the airflow path can become nearly or completely blocked.

As a result of the frost accumulation, refrigeration systems currently used in the industry are often oversized by about 50% compared to the case where no frost is grown, while the average energy input is 25% greater than the same system with no frost accumulation [1] .

The design and thermal selection of the heat exchangers have been extensively studied by Kakac et al. [2,3].

Sahin1 [4] and many other researchers noticed a linear relationship between frost height and time for the crystal growth stage. As a result, many linear growth models have been developed to explain early growth. One such model predicts the thermal conductivity of developing frost Sahin2 [5]. The frost is modeled as individual ice crystals that grow as columns. Thermal conductivity is given as a function of cold plate temperature, air temperature, Reynolds number, and absolute humidity.

Chen et al. [6,7] developed a more detailed numerical model to simulate frost growth on plate-fin heat exchangers for typical freezer conditions. Recently there have been more studies on ways to improve the performance of plate-fin - round-tube heat exchangers typically used for refrigerators and heat pump air conditioners under frosted conditions Ogawa et al.[8]. Recently, Seker et al.[9] presented a semi-empirical model to simulate frosting in commercial refrigerators. Although their numerical model simulates heat and mass transfer equations similar to those used by Verma et al.[10], it was semi-empirical and developed for refrigerators.

The model in this paper employs a finite volume and quasi-steady approach. The finite-volume approach helps overcome the scarcity of heat transfer and pressure drop correlations for fin-and-tube heat exchangers used in domestic refrigerators working under forced convection. The mass and heat transfer laws were used to predict the

frost growth characteristics. It is possible to extend available correlations and apply them to finite volumes without making too many assumptions. Also use of the finite volume technique makes it possible to model local frost deposition within the heat exchanger.

MODEL STRUCTURE AND ASSUMPTIONS

Figure (1) shows a schematic of a plain-fin-tube heat with aluminum fins and copper tubes. The dimensions of the heat exchanger are 500mm width, 100 mm height and 50mm depth, while the other specifications are listed in Table (1). It has six tube rows along the airflow direction and seven cross counter flow refrigerant circuits perpendicular to the airflow direction. The frost formation process involves simultaneous heat and mass transfer during varying thermophysical properties. This process is very complex. Some assumptions were made, to simplify the analysis:

1. Frost distribution is homogeneous over the heat exchanger.
2. Problem is assumed to be quasi-steady-state.
3. Only one dimensional heat and mass transfer over the heat exchanger is assumed.
4. Frost thermal conductivity varies only with frost density.
5. Radiation heat transfer between moist air and frost layer is negligible.

This assumption eliminates the need to model the complex early crystal growth period. The effect of frost surface roughness effect on the surface area is also neglected because it is significant only in the early stage. Also to speed convergence of the numerical solution, only the leading edge finite volume is assumed to contain a superheated segment.

Table (1) Geometric specifications of heat exchanger.

Fin thickness, m	0.001
Space between fins, m	0.010
Fin width, m	0.048
Number of circuits	7
Numb Number of rows	6
Inner diameter of tube, m	0.008
Outer diameter of tube, m	0.01
Longitudinal tube spacing, m	0.016
Transverse tube spacing, m	0.014

NUMERICAL MODEL

Figure (2) shows a fin and tube surface covered with frost. The heat transfer modeling of the conduction through the frost is done by considering a lumped model (Verma et al. [10]). For each tube and fin segment, the one-dimensional sensible heat transfer rate equation was solved simultaneously with the air-side energy equation using the local properties of the moist air. The total (sensible plus latent) heat transfer was determined by solving simultaneously the equations for conduction through the frost layer, heat transfer from the tube to refrigerant and refrigerant-side energy equation.

Time-dependent performance was approximated by a quasi-steady process where calculations at one time step served as inputs for the next as shown in Figure (3). The

results from each 2-min time step (i.e. frost thickness) were used to update the heat exchanger geometry (fin thickness, tube diameter) for the next. Experiments by Carlson et al. [11] showed that the choice of 1 or 3 min had less than a 1% effect on the simulation results. Details of the solution algorithm outlined in Figure (3) are described below.

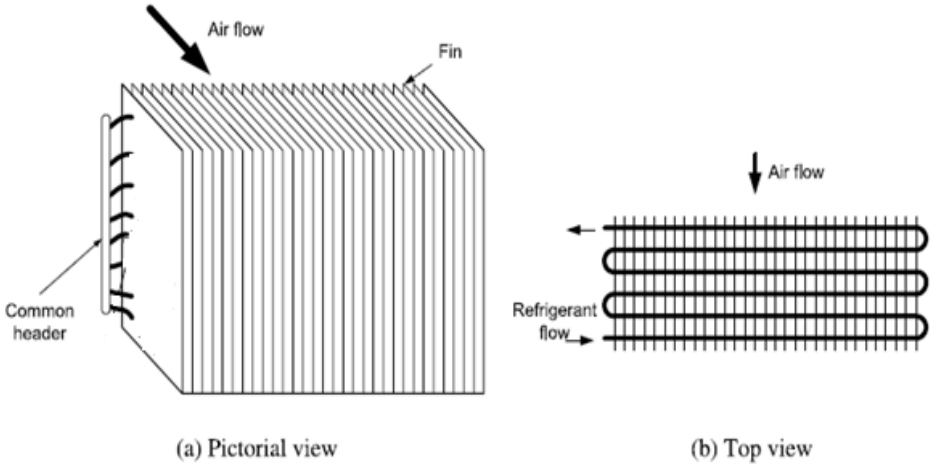

Figure (1) Schematic representation of heat exchanger.

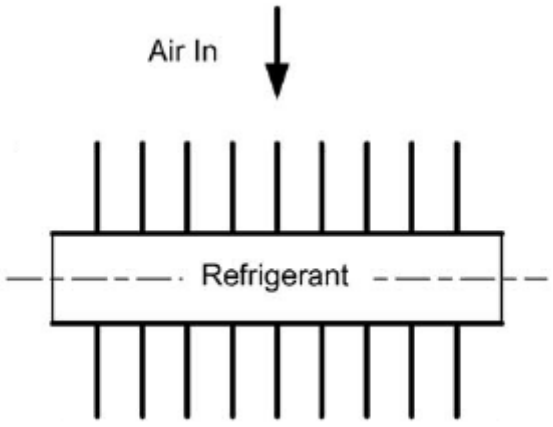

Figure (2) Frost formation on fin and tube.

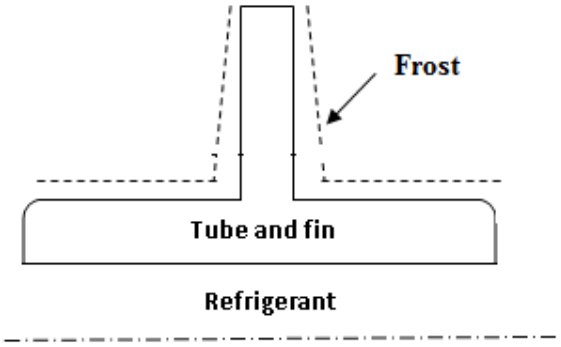

Figure (3) Structure of the model.

SEQUENCE OF CALCULATION

Air-side heat transfer coefficient

Kim correlation [12] is used to calculate the heat transfer coefficient, due to the range of geometric and operating parameters involved in this study.

$$h_a = j.G_{max}.c_{p,a}.Pr^{-2/3} \quad \ldots (1)$$

Where,

$$j = 0.16\,\mathrm{Re}^{-0.369}\left(\frac{S_T}{S_L}\right)^{0.106}\left(\frac{S_F}{D}\right)^{0.0138}\left(\frac{S_T}{D}\right)^{0.13} \quad \ldots (2)$$

Air- side pressure drop

Air side pressure drop is calculated by a correlation suggested by Kays and London [13],

$$\Delta P_a = \frac{G_{mas}^2}{2.\rho i}\left[\left(1+\sigma^2\right)\left(\frac{\rho_i}{\rho_e}-1\right)+ f.\frac{A_o}{A_{\min}}.\frac{\rho_i}{\rho_m}\right] \quad \ldots (3)$$

The friction factor contributions due to the fins and tube bank of the heat exchangers are used following Kim et al. [12]as,

$$f = 1.4356\,\mathrm{Re}_D^{-0.526}\left(\frac{S_T}{S_L}\right)^{-0.365} + \left(\frac{S_F}{D}\right)^{-0.131}\left(\frac{S_T}{D}\right)^{0.122} \quad \ldots (4)$$

Refrigerant side heat transfer coefficient

Gnielinski's [14] correlation for fully developed turbulent flow in a circular tube was used,

$$Nu = \frac{(f/8)(\mathrm{Re}-1000)\,\mathrm{Pr}}{1+12.7(f/8)^{1/2}(\mathrm{Pr}^{2/3}-1)} \quad \ldots (5)$$

$$h_r = \frac{Nuk_r}{D_h} \quad \dots (6)$$

Fin surface efficiency and the overall heat transfer coefficient

The fin surface efficiency is calculated using the Incropera and Dewitt [15],

$$\eta_s = 1 - \frac{A_f}{A_o}.\left(1 - \eta_f\right) \quad \dots (7)$$

Karatas [16] used the finite element method to solve this problem and correlated the fin efficiency as,

$\eta_f = -3.429.m^4+6.457m^3-4.308m^2+0.736.m+0.949$ …(8)

Where m, dimensionless fin factor is defined as,

$$m = \sqrt{\frac{2h_a}{k_{fin}.Fin_{th}}} \quad \dots (9)$$

The overall heat transfer coefficient of the evaporator can be calculated as,

$$UA_o = \left(\frac{1}{\eta_s.h_a.A_o} + \frac{1}{h_i A_i} + \frac{\delta_{fr}}{k_{fr}.A_o} \right)^{-1} \quad \dots (10)$$

Heat and mass transfer

Within each finite volume a set of simultaneous equations as follows quantify the energy and mass transfer rates from moist air to the refrigerant through the frosted fins and tubes. The cross-counter flow configuration links all these non-linear equations into a larger simultaneous set.

$Q_{sens,fin}=h_aA_o(T_{a,av}-T_{so,f})$ … (11)

$Q_{sens,tube}=h_aA_o(T_{a,av}-T_{so,tb})$ … (12)

$Q_{sens}=Q_{sens,fin}+Q_{sens,tube}$ …(13)

$Q_{sens}=m_{air}\ cp_{,a}(T_{a,in}-T_{a,out})$ … (14)

$Q_{lat,fin}=m_{fr,fin}\ \Delta h_{sg}$ … (15)

$Q_{lat,tube}=m_{fr,tube}\Delta h_{sg}$ … (16)

$Q_{lat}=Q_{lat,fin}+Q_{lat,tube}$ …(17)

$Q_{fin}=Q_{sens,fin}+Q_{lat,fin}$ … (18)

$Q_{tube}=Q_{sens,tube}+Q_{lat,tube}$ … (19)

$Q_{fr,fin}=Q_{fin,si}$ …(20)

$Q_{fin}=Q_{fr,si}+Q_{f,si}$ … (21)

$$Q_{tube} = k_{fr,tube} 2N_{tube}\pi(W - N_{fin}Fin_{th}) \frac{(T_{so,tube} - T_{si})}{\left(\ln\left(\frac{D_c}{D_{so}}\right)\right)} \quad \dots (22)$$

$Q_{total}=Q_{fin}+Q_{tube}$ … (23)

$Q_{total}=h_{ref}A_r(T_{si}-T_{r,av})$ … (24)

$Q_{total}=Q_{sens}+Q_{lat}=m_{ref}cp_{,r}(T_{r,in}-T_{r,out})$ … (25)

The mass transfer rate is calculated by solving simultaneously the continuity and the one-dimensional mass transfer equations for fins and tubes separately for each of the finite volumes.

$m_{fr} = m_{air} (w_{in} - w_{out})$ … (26)

$m_{fr} = (h_a \times Le^{-2/3} / cp,_a) \times A_o \times (w_{av} - w_{so})$ … (27)

Frost density

Hayashi [17] empirical correlation is used to determine frost density when the frost surface temperature is below freezing.

$$\rho_{fr}=650e^{0.277T} \quad \ldots(28)$$

The lower limit of −10 °C is not encountered when in modeling medium temperature display case evaporators for reasonable run times. However, to ensure robustness of the Newton–Raphson solution algorithm, a constant frost density is assumed below −10 °C. The more serious limitation of this correlation arises when the frost surface temperature rises to freezing temperature (0 °C), for a particular finite volume. This leads to repeated cycles of melting and refreezing, (Raju and Sherif [18]). The complexity of the structural changes of the frost along with the lack of definitive literature forces a simplifying assumption. For any finite volume where the frost surface temperature reaches the freezing point, Hayashi's correlation predicts a value of 650 kg/m^3, which is lower than the density of ice at 0 °C (920 kg/m^3). In this model the frost density is assumed to increase as water seeps continuously into the porous frost layer, continuously increasing its density to that of ice while the frost thickness remains constant.

Frost conductivity

The thermal conductivity of frost was determined as a function of density by employing the Yonko and Sepsy [19] correlation:

$$k_{fr}= (0.02422+7.214*10^{-4}\rho_{fr}+1.1797*10^{-6}\rho_{fr}^{2})/1000 \quad \ldots(29)$$

The correlation is limited to ρ_{fr}<576 kg/m^3. However, their correlation when extrapolated to the density of ice predicts the actual thermal conductivity of ice within 10%, so it is used for entire range of frost densities encountered.

Frost thickness

The thickness of the frost layer was computed by dividing the accumulated frost mass by the product of average frost density and surface area and neglecting any variation of frost density normal to the frost layer.

$\delta_{fr} = m_{fr} / (\rho_{fr} \times A_{o,dry})$ … (30)

Using the frost thickness, the heat exchanger geometry was updated and simulations proceeded to the next time step as shown in Figure (3).

RESULT AND DISCUSSION

The present study proposes a mathematical model using correlations for the heat transfer coefficients of the air-flow and a diffusion equation for the water–vapor in order to predict the frosting behavior on a fin–tube heat exchanger. To establish the

mathematical model, Table (2).shows the operating conditions that used in this study. The frost deposition pattern depends on the geometry of the heat exchanger and operating conditions.

Table (2) Parameters and their typical values for running conditions.

Operating conditions	Typical values
Air inlet temperature (°C):	-5, -10,-15
Refrigerant inlet temperature (°C)	-20,-25,-30
Air inlet RH	60%
Air velocity (m/s)	0.9
Refrigerant mass flow rate(kg/s)	0.5

Effect of inlet air temperature on frost thickness, pressure drop and total heat transfer coefficient

Three different air inlet temperature conditions were performed (-5,-10,-15) °C to see the effects of the air inlet temperature on frost thickness ,pressure drop and total heat transfer coefficient respectively as shown in Figures (4, 5, and 6). It can be seen from these figures that increase in inlet air temperatures increases the total heat transfer coefficient, air side pressure drop and frost thickness.

Effect of refrigerant temperature on frost thickness, pressure drop and total heat transfer coefficient

Three different surface temperatures (-20,-25,-30) °C were investigated numerically. As can be seen from these Figures (7, 8, and 9), the frost thickness, air side pressure drop and total heat transfer coefficient increase for
Lower refrigerant temperatures.

Effect of inlet air temperature and refrigerant temperature on total heat transfer load

The effect of inlet air temperature (-5,-10,-15) °C and refrigerant temperature (-20,-25,-30) °C on total heat transfer (sensible and latent) from moist air to the surface of fins and tubes heat exchanger were indicated in Figures (10&11). It can be noticed from these Figures that the decrease in the capacity of the heat exchanger with time for both cases.

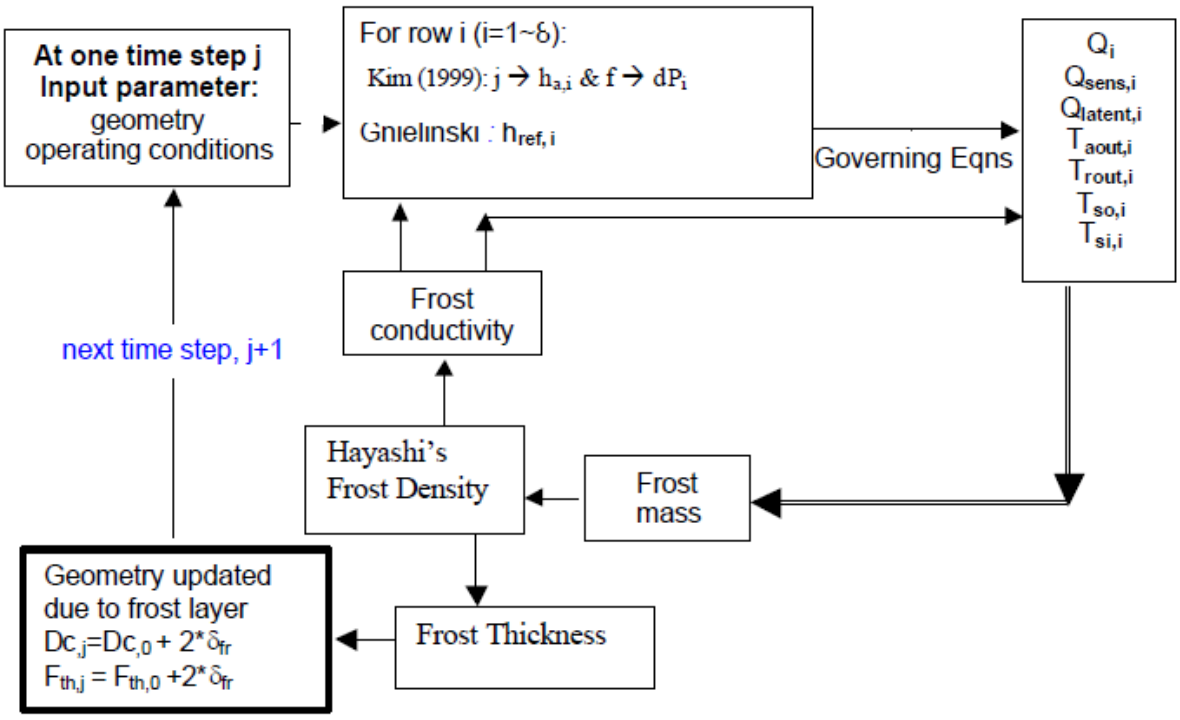

Figure (4) Structure of the model.

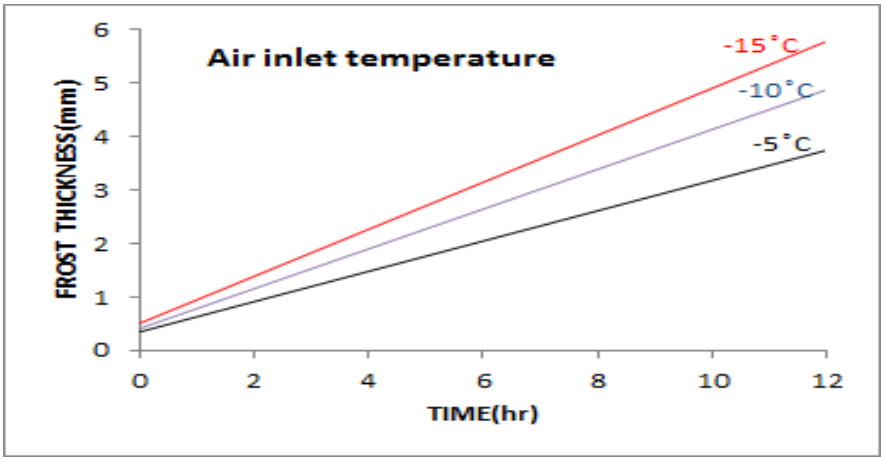

Figure(5) The change of frost thickness of heat exchanger for different inlet air temperatures.

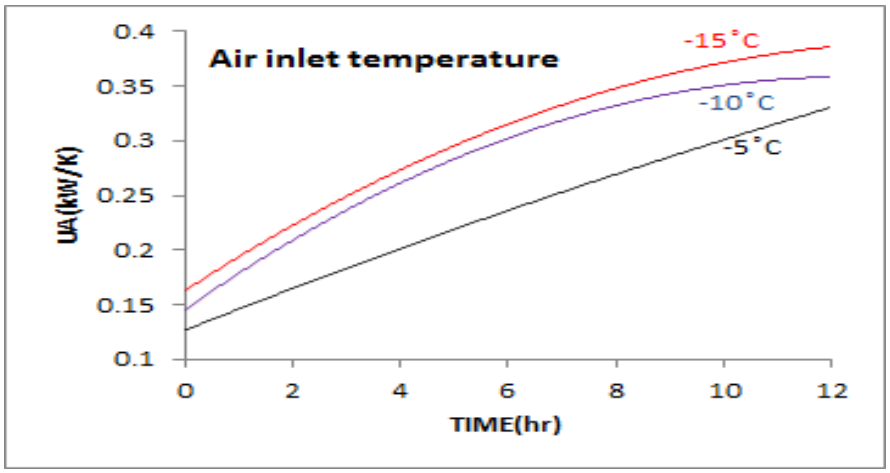

Figure(6) The change of total heat transfer coefficient of heat exchanger for different inlet air temperatures.

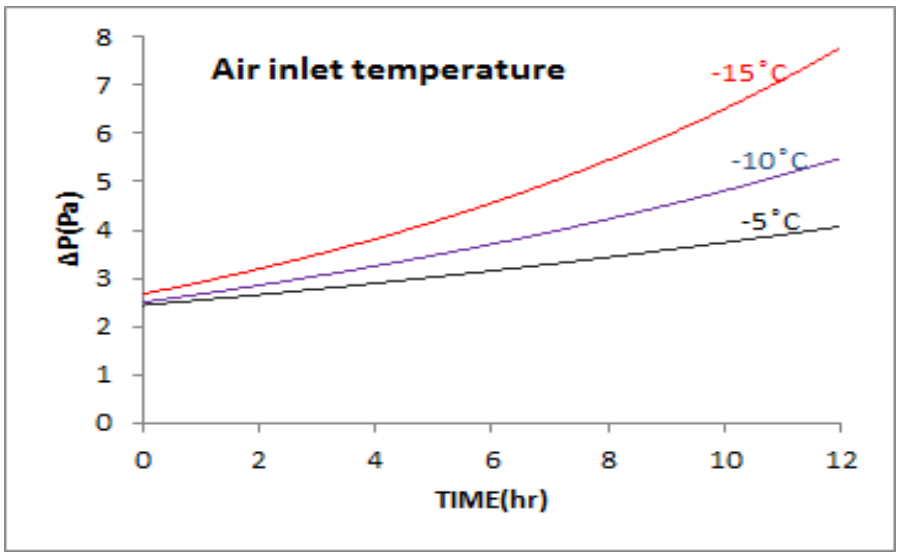

Figure(7) The change of air side pressure drop of heat exchanger for different inlet air temperatures.

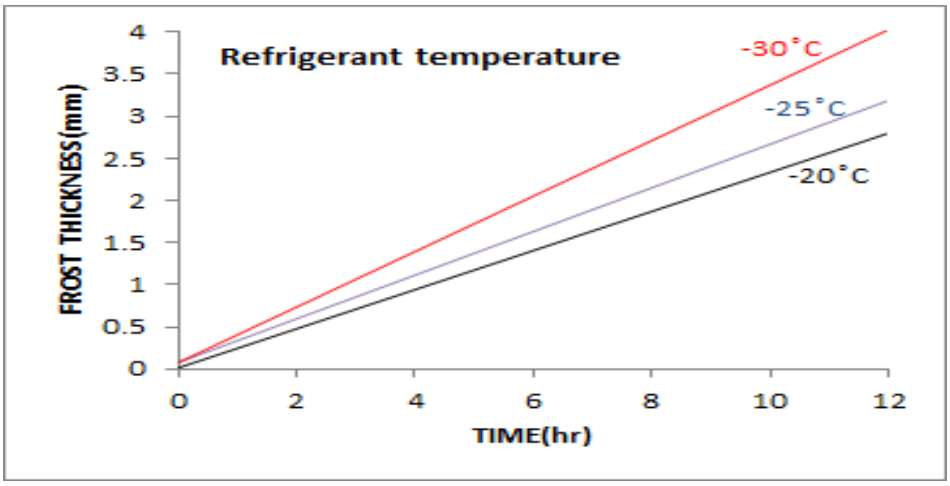

Figure(8) The change of frost thickness of heat exchanger for different inlet air temperatures.

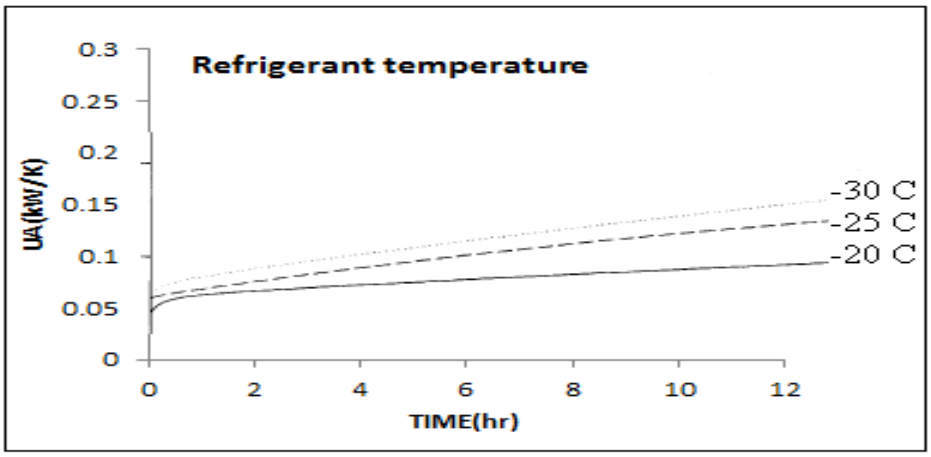

Figure(9) The change of total heat transfer coefficient of heat exchanger for different refrigerant temperatures.

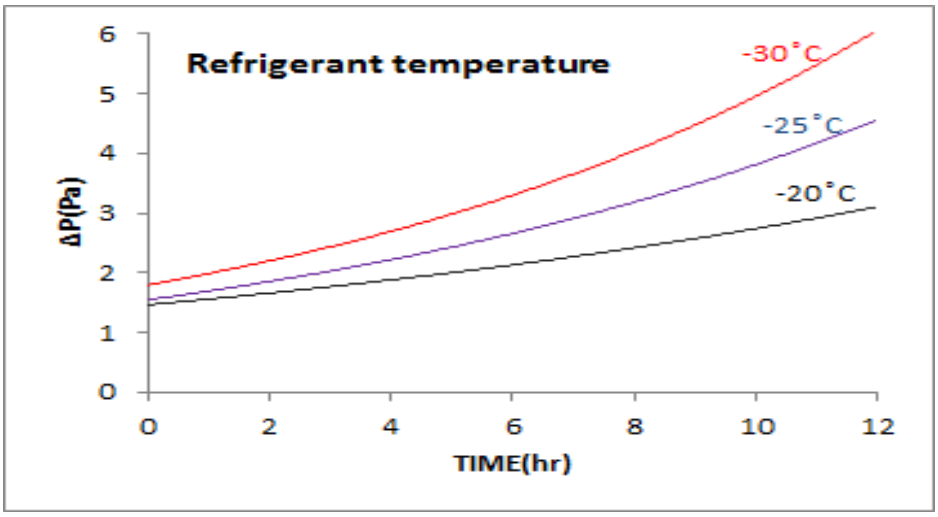

Figure(10) The change of air side pressure drop of heat exchanger for different refrigerant temperatures.

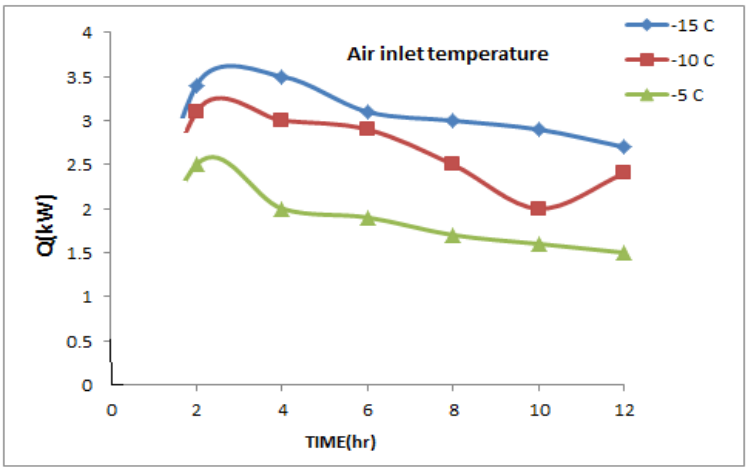

Figure(11) The change of total heat transfer load of heat exchanger for different refrigerant temperatures.

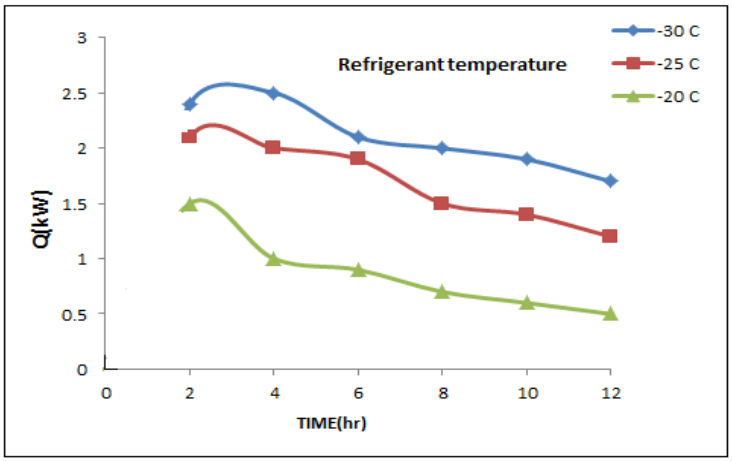

Figure(12) The change of total heat transfer load of heat exchanger for different air inlet temperatures. **Model validation of frost mass and thickness**

The present simulation model is developed for heat exchanger that is commonly used in supermarket refrigeration systems. Hence, the present quasi-steady state model of the frost is validated against the experimental data taken by C.W.Bullard et al. [20] for the case when the air inlet temperature (-10ºC), the refrigerant temperature (-25ºC), and the air velocity (0.9m/s). Figure (12) compares the predicted frost mass to that obtained from the experiment, the present model found to be agree well with frost mass from literature in the applicable geometries. The validation of frost thickness is illustrated in Figure (13) for the same literature [20] and for the same operating conditions. The model predicted frost thickness has an error of 15% at the beginning of frost growth as compared to that of the measured frost thickness.

CONCLUSIONS

This paper presented a mathematical model for fin and tube heat exchanger under frosted condition based on various empirical correlations of heat transfer coefficients and frost properties in order to predict the frost thermal conductivity and the amount of frost mass accumulation. The model was capable of predicting frost thickness, overall heat transfer coefficient and air side presser drop of heat exchangers. The results of the proposed model accurately predicted the frost growth and heat transfer rate and agreed well with the experimental data. This implies that the model can be used to predict the thermal performance of a fin–tube heat exchanger with multiple columns and rows.

REFERENCES

[1]. Chandrasekhar, an, R. C. Bullard, Analysis of design tradeoffs for display case evaporators, ORNL/TM-2004/157, Oak Ridge National Laboratory, Oak Ridge TN; 2004.

[2]. Kakac S, Liu H. Heat exchangers-selection, rating and thermal design, 2nd ed. Boca Raton, Florida, USA: CRC Press; 2002.

[3]. Kakac S. Boilers, evaporators and condensers, chapter 12. New York, USA: John Wiley; 1991.

[4].Sahin, A. Z.. "An Experimental Study on the Initiation and Growth of Frost Formation on a Horizontal Plate." Experimental Heat Transfer **7**: 101-119, 1994.
[5].Sahin, A. Z.. "Effective Thermal Conductivity of Frost during the Crystal Growth Period." International Journal of Heat and Mass Transfer 43: 539-553, 2000.
[6].Chen, H., Thomas, L. and Besant, R. W.. "Modeling Frost Characteristics on Heat Exchanger Fins: Part I, Numerical Model." ASHRAE Transactions 106 (2): 357-367, 2000a.
[7].Chen, H., Thomas, L., Besant, R. W.. "Modeling Frost Characteristics on Heat Exchanger Fins: Part II, Model Validation and Limitations." ASHRAE Transactions 106 (2): 368-376, 2000b.
[8]. Ogawa K, Tanaka N, Takeshita M. Performance improvement of plate fin and-tube heat exchangers under frosting conditions. ASHRAE Transactions Symposium CH 1993; 93-2-4.
[9]. Seker, D. Frost formation on fin-and-tube heat exchangers. Part I-modeling of frost formation on fin-and-tube heat exchangers, Int J Refrigeration 27 (4) (2004) 367–374.
[10]. Verma, P. C.W. Bullard, P.S. Hrnjak, Design tool for display case heat exchanger frosting and defrosting, University of Illinois at Urbana-Champaign, College of Engineering Library, ACRC Technical Report 201; 2002.
[11]. Carlson, D.M. P.S. Hrnjak, C.W. Bullard, Deposition, distribution, and effects of frost on a multi-row heat exchanger performance, University of Illinois at Urbana-Champaign, College of Engineering Library, ACRC Technical Report 183; 2001.
[12].Kim, N. H., Youn, B., and Webb, R. L. 1999. Air-Side Heat Transfer and Friction.
[13]. Kays WM, London AL. Compact heat exchangers, 3rd ed. Singapore: McGraw Hill; 1992.
[14]. Gnielinski, V. New equations for heat and mass transfer in turbulent pipe and channel flow, Chem Eng 16 (1976) 359–368.
[15]. Incropera P, DeWitt, P, 1990. Introduction to heat transfer, 2nd.
Correlations for Plain Fin-and- Tube Heat Exchangers with Staggered Tube Arrangements. Transactions of ASME, 121:662-667.
[16]. Karata و H, 1995. Theoretically and experimentally investigation
of a domestic refrigerator evaporator, MSc Thesis,Technical University of Istanbul-Institute of Science and Technology, Y´ stanbul.
[17]. Hayashi, Y. A. Aoki, S. Adachi, K. Hori, Study of frost properties correlation with frost formation types, J Heat Transfer 99 (1977) 239–245.
[18]. Raju, S.P. S.A. Sherif, Frost formation and heat transfer on circular cylinders in cross-flow, Int J Refrigeration 16 (3)(1993) 390–402.
[19]. Yonko, J.D. C.F. Sepsy, An investigation of the thermal conductivity of frost while forming on a flat horizontal plate,ASHRAE Trans 73 (II) 1967) I.1.1–I.1.11.
[20]. Bullard, C. W. P. S. Hrnjak, Experimentally validated model for frosting of plain fin round tube heat exchangers, IIF - IIR – Commission D1/B1 – Urbana, IL, USA – 2002.